INVESTIGATIVE REPORT

Combination Treatment with Human Adipose Tissue Stem Cell-derived Exosomes and Fractional CO_2 Laser for Acne Scars: A 12-week Prospective, Double-blind, Randomized, Split-face Study

Hyuck Hoon KWON[1], Steven Hoseong YANG[2], Joon LEE[1], Byung Cheol PARK[3], Kui Young PARK[4], Jae Yoon JUNG[1], Youin BAE[5] and Gyeong-Hun PARK[5]

[1]Oaro Dermatology Institute, Seoul, Republic of Korea, [2]Guam Dermatology Institute, Guam, USA, [3]Department of Dermatology, Dankook University, College of Medicine, Cheonan, [4]Department of Dermatology, Chung-Ang University, College of Medicine, Seoul, and [5]Department of Dermatology, Dongtan Sacred Heart Hospital, Hallym University College of Medicine, Hwaseong, Republic of Korea

A variety of applications of human adipose tissue stem cell-derived exosomes have been suggested as novel cell-free therapeutic strategies in the regenerative and aesthetic medical fields. This study evaluated the clinical efficacy and safety of adipose tissue stem cell-derived exosomes as an adjuvant therapy after application of fractional CO_2 laser for acne scars. A 12-week prospective, double-blind, randomized, split-face trial was performed. A total of 25 patients received three consecutive treatment sessions of fractional CO_2 laser to the whole face, with a follow-up evaluation. Post-laser treatment regimens were applied; for each patient, one side of the face was treated with adipose tissue stem cell-derived exosomes gel and the other side was treated with control gel. Adipose tissue stem cell-derived exosomes-treated sides had achieved a significantly greater improvement than the control sides at the final follow-up visit (percentage reduction in échelle d'évaluation clinique des cicatrices d'acné scores: 32.5 vs 19.9%, $p < 0.01$). Treatment-related erythema was milder, and post-treatment downtime was shorter on the human adipose tissue stem cell-derived exosomes-treated side. In conclusion, the combined use of this novel material with resurfacing devices would provide synergistic effects on both the efficacy and safety of atrophic acne scar treatments.

Key words: adipose tissue stem cell-derived exosomes; acne scar; fractional laser.

Accepted Oct 15, 2020; Epub ahead of print Oct 19, 2020

Acta Derm Venereol 2020; XX: XX–XX.

Corr: Gyeong-Hun Park, Department of Dermatology, Dongtan Sacred Heart Hospital, Hallym University College of Medicine, 7, Keunjae-bong-gil, Hwaseong-si, Gyeonggi-do 18450, Republic of Korea. E-mail: borelalgebra@gmail.com

SIGNIFICANCE

Adipose tissue stem cell-derived exosomes possess the critical properties of mesenchymal stem cells in the repair of organ injuries. Furthermore, adipose tissue stem cell-derived exosomes can avoid the risks of stem cell therapy because they are cell-free. A double-blind, randomized, first-in-human, clinical trial was conducted to evaluate the efficacy and safety of highly purified adipose tissue stem cell-derived exosomes as an adjuvant therapy after fractional CO_2 laser application for acne scars. Application of adipose tissue stem cell-derived exosomes treatment yielded more favourable responses, a shorter recovery time, and fewer side-effects. The combined use of adipose tissue stem cell-derived exosomes with resurfacing devices could provide synergistic effects on the efficacy and safety of atrophic acne scar treatments.

Facial atrophic acne scarring is a psychologically damaging condition that can cause social disability. Fractional laser resurfacing has widened therapeutic options and has become the current standard of care (1–3). While ablative fractional carbon dioxide laser (FCL) resurfacing has demonstrated clinical efficacy in acne scar treatment, patients still need better improvement of scars and sustain side-effects during post-procedural wound healing (4). Therefore, an adjuvant application of adipose-derived stem cell (ASC)-conditioned medium (CM) has been tried, with synergistic effects in augmenting treatment responses and reducing adverse effects through its potential to accelerate tissue regeneration and wound healing (5).

Because mesenchymal stem cells (MSCs) can differentiate into various cell types as multipotent stem cells, their unique self-renewal capacities have made them a promising cell-based therapy to treat several human diseases (6). However, there have been several drawbacks in the use of MSCs, such as poor engraftment efficiency, potential tumour formation, and difficulty in quality control (7). Furthermore, paracrine signalling of MSCs is reported to be essential for their beneficial effects on tissue regeneration and anti-inflammation.

Exosomes are lipid bilayer-enclosed extracellular vesicles, 30–200 nm in diameter, produced by almost all cells and present in all body fluids (8–10). They are regarded as an essential mediator of intercellular communication by transferring proteins and genetic material between cells (9). Several studies have shown that MSC-derived exosomes carry the essential properties of MSCs (11–13), suggesting that exosomes may be a compelling alternative to MSCs in regenerative and aesthetic medicine, as they would avoid most of the problems associated with live MSC-based therapy (14). Interes-

tingly, recent studies have shown that human adipose tissue stem cell-derived exosomes (ASCE) possess the critical properties of stem cells and are as potent as MSCs in the repair of various organ injuries (15, 16). In fact, a variety of applications for ASCE have been suggested as novel cell-free therapeutic strategies in regenerative and aesthetic medicine. These data strongly suggest the suitability of ASCE as an adjuvant treatment modality in combination with FCL for the treatment of acne scars.

Since most single treatment modalities for acne scars yield less than ideal results with regard to efficacy and safety, customized combination treatments with various therapeutic methods are needed for optimal outcomes. Therefore, the aim of this study was to evaluate the clinical efficacy and safety of ASCE as an adjuvant therapy after application of FCL for acne scars.

MATERIALS AND METHODS

Study design and patient enrollment

A 12-week prospective, double-blind, randomized, split-face, comparative study was conducted to evaluate the clinical efficacy of application of ASCE after FCL in the treatment of facial acne scars. The study was carried out in accordance with the Declaration of Helsinki and approved by our institutional review board. Informed consent was obtained from all subjects prior to enrollment. In this study, patients received 3 consecutive treatments of FCL on their whole face at an interval of 3 weeks, with a follow-up evaluation 6 weeks after their final treatment session. An independent researcher created the random allocation sequence by a computer-based random number generator, using block randomization with a block size of 4 to assign the post-laser treatment modality of each half of the face between ASCE and control gel. The allocation was concealed from subjects and investigators, and was preserved by using sequentially numbered, sealed envelopes.

Twenty-five Korean subjects (18 men and 7 women, age range 19–54 years, 12 with Fitzpatrick skin type III and 13 with type IV) with atrophic acne scars were enrolled between October and November 2019. The sample size was determined based on feasibility, because previous data for power analysis were not available. Patients whose échelle d'évaluation clinique des cicatrices d'acné (ECCA) scores were 50 or higher were eligible for inclusion (17). Patients were excluded from the study if they had active acne under treatment or if they had received any other treatments for acne scars during the 12 months prior to the first treatment. Other treatments, including chemical, mechanical, or laser resurfacing, were not permitted during the study period.

Exosome purification and preparation of adipose tissue stem cell-derived exosomes gel for clinical application

Exosomes in this study were acquired from human ASC-CM by ExoSCRT™ technology (ExoCoBio Inc., Seoul, Republic of Korea) as described previously (18). Briefly, CM was collected from ASCs cultured with serum-free Dulbecco's Modified Eagle's Medium (Thermo Fisher Scientific, Waltham, MA, USA) in a 5% CO_2 atmosphere at 37°C. Collected CM was filtered through a 0.2-μm filter to remove non-exosomal particles. Exosomes were further concentrated and purified by tangential-flow filtration with a 500-kDa molecular weight cut-off filter membrane cartridge. Quantification of exosomes was performed by nanoparticle tracking analysis (NTA).

ASCE were prepared as gel solutions at 2 different doses for clinical application. To prepare the ASCE gel, ASCE were prepared at 9.78×10^{10} particles/ml (for the day of FCL treatment) or 1.63×10^{10} particles/ml (for days subsequent to FCL treatment) in a gel solution containing 30% ASCE. Detailed information on the ASCE and control gel solution is described in Appendix S1[1]. To maintain blinding of investigators and subjects, the ASCE and control gel solutions were prepared with identical syringes, labelled left and right.

Treatment protocol

The entire face of each patient was treated with 10,600-nm FCL (Fraxis, Ilooda, Suwon, Korea). The face was cleansed with mild soap and topical anaesthesia was applied using EMLA® cream (Astrazeneca, Södertälje, Sweden) to the entire face under occlusion for 30 min prior to laser therapy. The treatment parameters were determined based on each patient's condition and availability as follows: 7.2–9.0 mJ, 240–300 μs duration, and 0.8–1.0 mm density in FCL (coverage=20–25%, each pixel size=100 μm, and approximate depth=1,100–1,400 μm, treatment density 120–160 microthermal zones/cm^2). Each treatment session encompassed the entire face for two passes.

Post-laser treatment regimens were applied as follows: all patients were treated with 1 ml of either ASCE gel or control gel on each half of the face according to random assignment just after finishing the laser treatment. For the next two consecutive days after each treatment, patients were instructed to apply each solution to the designated half of the face twice a day as described.

Clinical outcome assessment

All patients were photographed using a standardized digital camera (EOS 600D, Canon, Tokyo, Japan) under identical lighting conditions at each visit. Efficacy of scar improvement was assessed by the ECCA score at each visit, as well as the Investigator's Global Assessment (IGA) at the final follow-up visit (17). IGA was evaluated using a 5-point scale associated with the degree of improvement (grade 0=no improvement, 1=1–25% improvement, 2=26–50% improvement, 3=51–75% improvement, and 4=76–100% improvement) (19, 20). For ECCA scoring, atrophic acne scars were classified into specific subtypes including icepick (V-shaped), boxcar (U-shaped), and rolling scar (M-shaped) according to their shape and size (17, 21), and the ECCA score was determined according to the number of each subtype of scar, as previously described (17). Two experienced dermatologists rated ECCA scores and IGA on the basis of the photographs in a fully blinded manner. The primary efficacy outcome was the percentage change in total ECCA score at the final follow-up visit. Secondary outcomes were the percentage change in total ECCA at weeks 3 and 6, the change in ECCA score for each subtype of atrophic scar at weeks 3, 6, and 12, and IGA at week 12.

Meanwhile, patients recorded the post-treatment responses, including erythema, oedema, and dryness with a 0–3 severity scale (0=none, 1=mild, 2=moderate, and 3=severe), daily for 7 days after each treatment session. Daily pain scores for the first post-treatment week were also recorded with a 0–10 severity scale (0 for no pain, 10 for the worst imaginable pain) during each post-treatment period. Other post-procedural complaints, including hyperpigmentation and secondary scarring, were documented at the final follow-up visit. The overall duration of subjective downtime, defined as the time during which the patient felt that treatment meaningfully affected their quality of life, was also recorded after each treatment session.

[1]https://www.medicaljournals.se/acta/content/abstract/10.2340/00015555-3666

Three-dimensional (3D) image analysis

To provide supportive data for the objective evaluation of treatment efficacy, a 3D camera and software (Antera 3D® CS, Miravex, Dublin, Ireland) were used for 4 patients. Antera 3D® captures high-resolution images and provides images in 3 dimensions using optical methods and complex mathematical algorithms, which makes it possible to extract and quantify data on the 3-dimensional shape of the skin. The depressed volume of atrophic scars, mean volume of skin pores, and skin surface roughness at the selected area were objectively measured at each visit.

Statistical analysis

Baseline characteristics were presented as the mean ± standard deviation (SD) and range for continuous variables, and as number and percentage for categorical variables. Baseline data and IGA were analysed using the Wilcoxon signed-rank test to compare between treatment sides. Linear mixed effect models were used to analyse ECCA scores, atrophic scar volume, mean pore volume, and skin surface roughness. The duration of downtime was evaluated using a generalized linear mixed model with generalized Poisson family. Post-treatment pain, erythema, oedema, and dryness were assessed using cumulative link mixed models. The McNemar test was used to compare the occurrence of post-treatment hyperpigmentation and scar formation between treatment sides. A *p*-value less than 0.05 was considered statistically significant. All statistical analyses were performed using R version 3.6.2 (R Foundation for Statistical Computing, Vienna, Austria). Further details are provided in Appendix S1[1].

RESULTS

A total of 25 enrolled patients completed the study. Baseline patient characteristics are summarized in **Table I**. There were no significant differences in total ECCA score or scores of the 3 major subtypes (V-, U-, and M-shaped) of atrophic scars at baseline between the ASCE-treated and control sides.

Table I. Baseline characteristics of participants

Characteristics	ASCE side	Control side	*p*-value
Age, years, mean ± SD (range)	35.6 ± 8.2 (19–54)		
Sex, *n* (%)			
Male	18 (72)		
Female	7 (28)		
Fitzpatrick skin type, *n* (%)			
Type III	12 (48)		
Type IV	13 (52)		
ECCA score, mean ± SD (range)			
Total	88.4 ± 35.2 (50–180)	81.6 ± 33.0 (50–180)	0.14
V-type	31.2 ± 8.6 (15–45)	30.6 ± 8.1 (15–45)	> 0.99
U-type	35.2 ± 11.9 (20–60)	32.0 ± 11.5 (20–60)	0.13
M-type	22.0 ± 24.3 (0–75)	19.0 ± 24.2 (0–75)	0.50
Atrophic scar volume, mm^3	3.7 ± 1.9 (1.9–6.2)	4.4 ± 3.2 (2.4–9.1)	0.63
Pore volume, 10^{-3} mm^3, mean ± SD (range)	4.0 ± 0.8 (3.0–5.0)	3.8 ± 1.0 (3.0–5.0)	> 0.99
Skin surface roughness	10.7 ± 2.3 (7.8–13.2)	10.2 ± 2.4 (6.7–11.7)	0.88

ASCE: adipose tissue stem cell-derived exosomes, ECCA: échelle d'évaluation clinique des cicatrices d'acné; SD: standard deviation.

Characterization of exosomes applied in clinical trial

ASCE were analysed with an NTA instrument to measure particle size distribution and concentration. As shown in **Fig. 1**A, the mode size was approximately 117.4 nm, and the concentration was 3.26×10^{11} particles/ml. Cryo-transmission electron microscopy analysis revealed ASCE that were spheres of 30–200 nm diameter and exhibited a clear lipid bilayer structure (Fig. 1B). Next, ASCE were stained with antibodies against well-established exosome surface markers (CD9, CD63, and CD81) and were analysed using bead-based flow cytometry. As shown in Fig. 1C, ASCE were positively stained with all 3 markers. The purity of the ASCE was determined by the absence of calnexin and cytochrome C, negative markers of exosomes. In line with the literature, ASCE exhibited low levels of calnexin and cytochrome C (Fig. 1D). To evaluate biological functions of ASCE in target cells, 4 *in vitro* potency assays were performed. As shown in Appendix S1; SFig. 1[1], ASCE increased collagen synthesis, cell migration and proliferation in human dermal fibroblast and decreased inflammatory cytokine level in murine macrophage. These results indicate that ASCE isolated by ExoSCRT™ technology exhibit typical characteristics of exosomes. Purified ASCE were used in ASCE solutions, and *in vitro* data were described in Appendix S1[1].

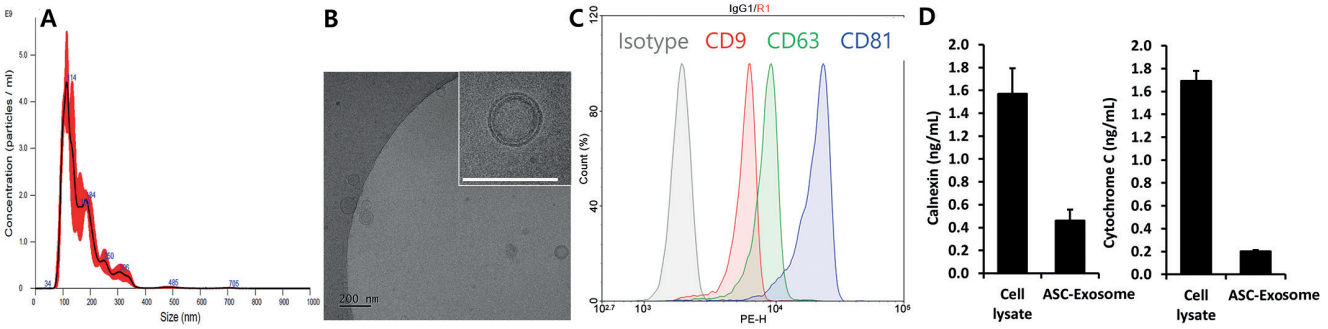

Fig. 1. Characterization of adipose tissue stem cell-derived exosomes (ASCE). (A) Representative plot of particle concentration and size distribution of ASCE, as measured by nanoparticle tracking analysis (NTA). (B) Cryo-transmission electron microscopy image of ASCE. *Scale bar*: 200 nm. (C) Signal intensities of exosome surface markers. ASCE were analysed using flow cytometry after staining with anti-CD9, -CD63, and -CD81 antibodies. (D) Levels of exosome exclusionary markers, calnexin and cytochrome C, in ASCE compared with cell lysate. Data are presented as the mean ± standard deviation (SD) of 3 independent experiments.

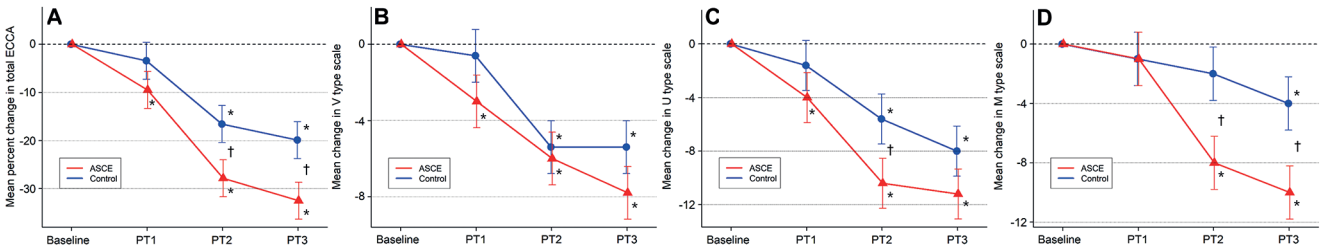

Fig. 2. Evaluation of scar improvement based on échelle d'évaluation clinique des cicatrices d'acné (ECCA) scores. (A) Mean percentage changes in total ECCA scores and mean changes in ECCA scores for (B) V-shaped (icepick), (C) U-shaped (boxcar), and (D) M-shaped (rolling) atrophic scars on the adipose tissue stem cell-derived exosomes (ASCE) and control sides. *$p < 0.05$ compared with baseline; †$p < 0.05$ between the 2 sides. Error bars indicate standard errors. PT: post-treatment.

Evaluation of scar improvement

A significant reduction in ECCA score from baseline was observed on the ASCE side beginning at the first post-treatment visit and on the control side from the second post-treatment visit (Fig. 2A). The difference in percent reduction of ECCA score between the two regimens was not significant at the first post-treatment visit, but became significant at the second post-treatment visit. At the final follow-up visit, the ECCA score was reduced by 32.5% (95% confidence interval [CI]: 24.8–40.2%) from baseline on the side treated with ASCE, which was significantly greater than the reduction of 19.9% (95% CI: 12.2–27.6%) on the control side ($p < 0.01$). Mean reductions in ECCA score were also analysed for each subtype (V-, U-, and M-shaped) of atrophic scar (**Fig. 2**B–D). For both V- and U-shaped scars, significant decreases in ECCA score from baseline were observed on both sides, but the differences in the reduction of ECCA score between the two regimens were not statistically significant at the final follow-up visit. For M-shaped scars, the ECCA score was significantly decreased compared with baseline on both sides, and ASCE-treated sides showed a significantly greater improvement than the control side at the final follow-up visit.

The IGA scores demonstrated comparable patterns to the ECCA evaluations. The grades 0, 1, 2, 3, and 4 were observed in 1, 8, 10, 5, and 1 facial sides treated with ASCE, respectively, and in 2, 11, 11, 1, and 0 facial sides with control, respectively. The ASCE-treated facial side demonstrated superior improvement based on IGA score compared with the control side after 3 sessions of each treatment ($p = 0.02$). Sixteen out of 25 facial sides achieved grade 2 or more improvements on the ASCE side, compared with 12 of the control-treated sides. **Fig. 3** shows a representative case before and after each application.

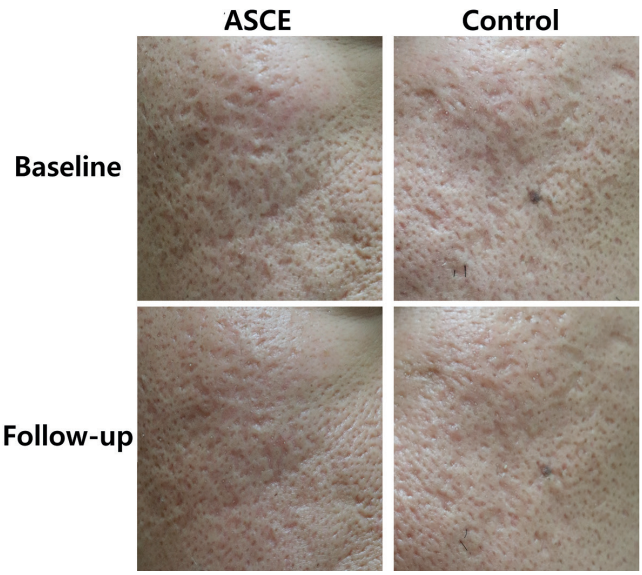

Fig. 3. Clinical photographs of the adipose tissue stem cell-derived exosomes (ASCE) and control sides at baseline and 6 weeks after 3 treatment sessions in a 30-year-old male.

Three-dimensional image analysis

The depressed volume of atrophic scars, mean volume of skin pores, and skin surface roughness were objectively measured using an Antera 3D® CS at baseline and post-treatment visits (**Fig. 4**). At the final follow-up visit, all of atrophic scar volume, mean pore volume, and skin surface roughness were significantly decreased from baseline on the ASCE side. In contrast, no significant decreases were observed on the control side.

Adverse effects

Various treatment-related side-effects, including post-treatment pain, erythema, oedema, and dryness, were experienced on both ASCE and control sides (**Figs 5** and **6**), but they were nearly resolved within 5 days. The severity of erythema during the first post-treatment week was significantly lower on the exosome side than on the control side ($p = 0.03$). Post-treatment pain, oedema, and dryness also tended to be milder on the exosome side, although not statistically significant. The mean duration of downtime was shorter on the ASCE side compared with the control side (4.1 (95% CI 3.5–4.8) days vs 4.3 (95% CI 3.7–5.1) days, $p = 0.03$). Two patients reported mild hyperpigmentation on the control side; one patient reported mild hyperpigmentation on the ASCE side ($p = 0.32$). No patient healed with scar formation or other permanent events.

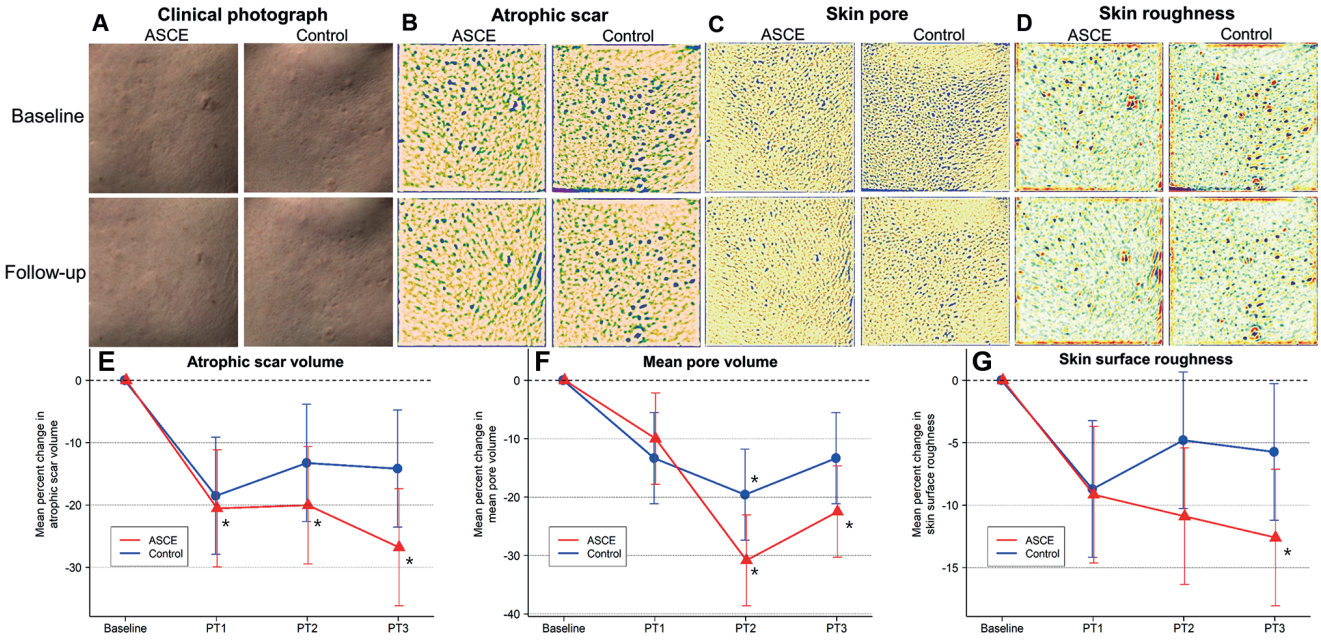

Fig. 4. Three-dimensional image analyses for atrophic scar, enlarged skin pore, and skin surface roughness using Antera 3D® CS. (A–D) Clinical photographs and analysed images of the adipose tissue stem cell-derived exosomes (ASCE) and control sides at baseline and at the final follow-up visit. (B) The depths of atrophic scars are shown as colours (white<yellow<green<blue<purple). (C) The depths of enlarged skin pores are shown as colours (white<yellow<orange<green<blue). (D) The vertical deviations of the skin surface are shown as colours: [downward] purple<blue<green<white <yellow<red [upward]. Mean percent changes in (E) atrophic scar volume, (F) mean pore volume, and (G) skin surface roughness on the ASCE and control sides. *$p < 0.05$ compared with baseline. Error bars indicate standard errors. PT: post-treatment.

DISCUSSION

Atrophic acne scars are associated with an incomplete recovery of the dermal matrix damaged by chronic inflammation (22, 23). Therefore, most fractional resurfacing devices work by depositing a pixilated pattern of microscopic wounds surrounded by healthy tissue, which are then repaired by the natural recovery process (24). However, the regenerative capability of these controlled wounds may be limited in many cases, frequently leading to delayed healing with unsatisfactory results. This specific period is also associated with various treatment-related complications, necessitating a clinical adjuvant application of soothing biological materials (25–27).

This split-face study demonstrates the clinical benefits of the postoperative application of ASCE for acne scars. To the best of our knowledge, this is the first study to use ASCE for human skin wound repair. The ASCE-treated side experienced significantly better improvement. Although both sides demonstrated steady improvement during treatment sessions, a significant difference between them was observed after completing the second session. Compared with other available adjuvant biological materials, the degree of additional improvement and relatively earlier onset time of ASCE were satisfactory (2, 4). The relative lack of efficacy of V- and U-subtypes suggests that the co-application of physical treatments including dot peeling or subcision is still needed with ASCE. From a safety perspective, ASCE-treated sides exhibited reduced post-procedural erythema and a shorter downtime.

When FCL is administered to the skin, the epidermis penetrated by the beams is instantly vaporized in micro-columns reaching down into the dermis; these columns

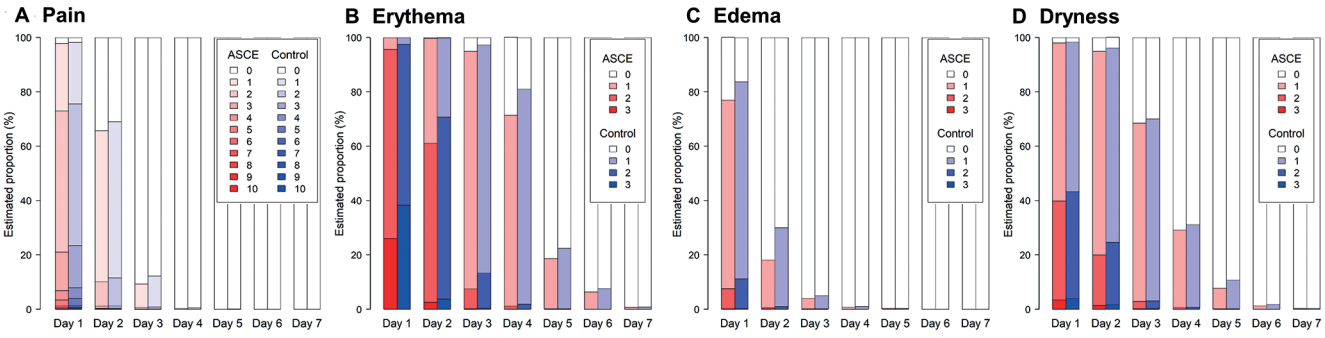

Fig. 5. Evaluation of: (A) pain, (B) erythema, (C) oedema, and (D) dryness on both adipose tissue stem cell-derived exosomes (ASCE) and control sides for post-treatment 7 days.

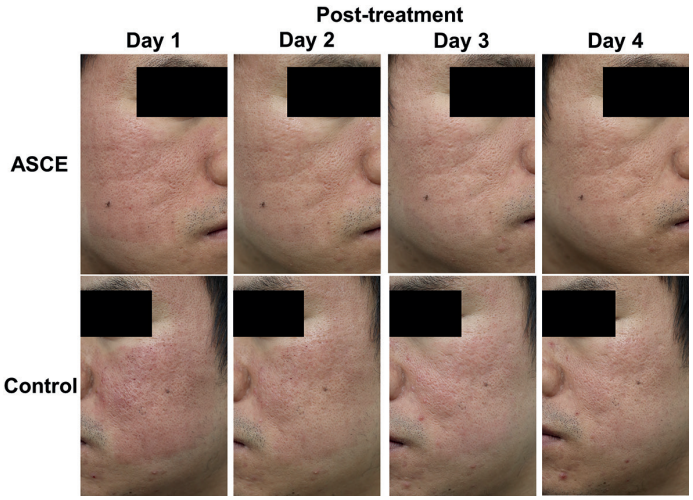

Fig. 6. Clinical photographs of the adipose tissue stem cell-derived exosomes (ASCE) and control sides for post-treatment 4 days in a 31-year-old male.

are called microablative columns (MACs) (28). MACs begin regeneration within several hours and complete re-epithelization is usually achieved within 2–3 days. During recovery, there is an accumulation of materials involved in wound remodelling, such as heat shock protein, procollagen, and dermal elastin (29). During this process, the temporarily formed vertical channel bypassing epidermal skin barriers allows an effective passage of microparticles, such as exosomes utilized in this study, into dermal tissues (30).

A mechanistic rationale for combining FCL and ASCE in acne scar treatment is the ability of ASCE to induce rapid healing after FCL ablation by supplying multiple anti-inflammatory and regenerative growth factors (31–35). Like ASCs, ASCE are also considered to optimize characteristics of fibroblasts, such as promoting the migration, proliferation, and collagen synthesis of fibroblasts (36–38), thereby accelerating wound healing of soft tissue with extracellular matrix remodelling (39, 40). ASCE also promote scarless cutaneous wound repair by regulating the ratios of collagen type III:type I, transforming growth factor (TGF)-β3:TGF-β1 and matrix metalloproteinase 3:tissue inhibitor of metalloproteinases-1, and by regulating fibroblast differentiation to mitigate scar formation (38). There is accumulating evidence that several signalling pathways related to skin regeneration and wound healing are stimulated by ASCE (34). A recent paper also demonstrates that ASCE can increase the *de novo* synthesis of ceramides to rebuild skin barrier (35). Compared with other biological materials, including platelet-rich plasma and stem cell-conditioned medium, ASCE have potential advantages as they are mass-produced, sterilized by filtration, and have a longer shelf-life.

As the exosomes used in this study were isolated from CM of ASCs from a healthy donor, there may be consideration of possible inter-individual variation. To make consistent functionality of exosomes, standardized quality control (QC) for cells and exosomes was applied. Various tests such as phenotype (surface markers, differentiation potential, etc.) and growth kinetics, for stem cell itself were performed to ensure the quality of cells as the source of exosomes (41), as previously recommended (42–44). More importantly, QC for exosomes were also performed to compare the functional activities of ASCE according to the recommendation of the Korean Ministry of Food and Drug Safety (45) and the International Society for Extracellular Vesicles (46). Through the QC, *in vitro* potency assays have shown consistent results with low variations.

Furthermore, no specific immunity concerns have been raised regarding MSC-derived exosomes. Like their cellular source, MSC exosomes are hypoimmunogenic (47). They are negative for major histocompatibility complex (MHC) class I and II, and co-stimulatory molecules, such as B7-1 (CD80), B7-2 (CD86) and CD40 (48, 49). ASCE, used in the present study, were also negative for the human leukocyte antigens (HLA), the human MHCs, such as HLA-ABC and HLA-DRDPDQ (35, 41). In addition, the immunologic safety of MSC exosomes has been confirmed through various *in vitro* and *in vivo* studies (50–54).

There were some limitations to this study. First, all enrolled patients had a similar ethnic background. Secondly, further studies pursuing optimal ASCE application regimens are necessary.

In conclusion, treatment with ASCE afforded more favourable responses, a shorter recovery time, and fewer side-effects when utilized in combination with FCL for acne scarring. Therefore, co-treatment with this novel material with resurfacing devices may provide synergistic effects on both efficacy and safety for atrophic scar treatments.

ACKNOWLEDGEMENTS

Exosome and control solutions used in this study were manufactured, purified and provided by ExoCoBio Inc. (Seoul, Korea).

The authors have no conflicts of interest to declare.

REFERENCES

1. Wat H, Wu DC, Chan HH. Fractional resurfacing in the Asian patient: current state of the art. Lasers Surg Med 2017; 49: 45–59.
2. Jordan R, Cummins C, Burls A. Laser resurfacing of the skin for the improvement of facial acne scarring: a systematic review of the evidence. Br J Dermatol 2000; 142: 413–423.
3. Bradley JA, Bolton EM, Pedersen RA. Stem cell medicine encounters the immune system. Nat Rev Immunol 2002; 2: 859–871.
4. Kwon HH, Park HY, Choi SC, Bae Y, Kang C, Jung JY, et al. Combined fractional treatment of acne scars involving non-ablative 1,550-nm erbium-glass laser and micro-needling

radiofrequency: a 16-week prospective, randomized split-face study. Acta Derm Venereol 2017; 97: 947–951.
5. Zhou BR, Zhang T, Bin Jameel AA, Xu Y, Xu Y, Guo SL, et al. The efficacy of conditioned media of adipose-derived stem cells combined with ablative carbon dioxide fractional resurfacing for atrophic acne scars and skin rejuvenation. J Cosmet Laser Ther 2016; 18: 138–148.
6. Shin TH, Kim HS, Choi SW, Kang KS. Mesenchymal stem cell therapy for inflammatory skin diseases: clinical potential and mode of action. Int J Mol Sci 2017; 18.
7. Lou G, Chen Z, Zheng M, Liu Y. Mesenchymal stem cell-derived exosomes as a new therapeutic strategy for liver diseases. Exp Mol Med 2017; 49: e346.
8. Thery C, Zitvogel L, Amigorena S. Exosomes: composition, biogenesis and function. Nat Rev Immunol 2002; 2: 569–579.
9. Colombo M, Raposo G, Thery C. Biogenesis, secretion, and intercellular interactions of exosomes and other extracellular vesicles. Annu Rev Cell Dev Biol 2014; 30: 255–289.
10. Kalluri R, LeBleu VS. The biology, function, and biomedical applications of exosomes. Science 2020; 367.
11. Golan K, Kumari A, Kollet O, Khatib-Massalha E, Subramaniam MD, Ferreira ZS, et al. Daily onset of light and darkness differentially controls hematopoietic stem cell differentiation and maintenance. Cell Stem Cell 2018; 23: 572–585 e577.
12. Pelizzo G, Avanzini MA, Icaro Cornaglia A, De Silvestri A, Mantelli M, Travaglino P, et al. Extracellular vesicles derived from mesenchymal cells: perspective treatment for cutaneous wound healing in pediatrics. Regen Med 2018; 13: 385–394.
13. Ferreira ADF, Cunha PDS, Carregal VM, da Silva PC, de Miranda MC, Kunrath-Lima M, et al. Extracellular vesicles from adipose-derived mesenchymal stem/stromal cells accelerate migration and activate AKT pathway in human keratinocytes and fibroblasts independently of miR-205 activity. Stem Cells Int 2017; 2017: 9841035.
14. Phinney DG, Pittenger MF. Concise review: MSC-derived exosomes for cell-free therapy. Stem Cells 2017; 35: 851–858.
15. Lai RC, Yeo RW, Lim SK. Mesenchymal stem cell exosomes. Semin Cell Dev Biol 2015; 40: 82–88.
16. Park JE, Tan HS, Datta A, Lai RC, Zhang H, Meng W, et al. Hypoxic tumor cell modulates its microenvironment to enhance angiogenic and metastatic potential by secretion of proteins and exosomes. Mol Cell Proteomics 2010; 9: 1085–1099.
17. Dreno B, Khammari A, Orain N, Noray C, Merial-Kieny C, Mery S, et al. ECCA grading scale: an original validated acne scar grading scale for clinical practice in dermatology. Dermatology 2007; 214: 46–51.
18. Cho BS, Kim JO, Ha DH, Yi YW. Exosomes derived from human adipose tissue-derived mesenchymal stem cells alleviate atopic dermatitis. Stem Cell Res Ther 2018; 9: 187.
19. Kravvas G, Al-Niaimi F. A systematic review of treatments for acne scarring. Part 1: Non-energy-based techniques. Scars Burn Heal 2017; 3: 2059513117695312.
20. Min S, Park SY, Moon J, Kwon HH, Yoon JY, Suh DH. Comparison between Er:YAG laser and bipolar radiofrequency combined with infrared diode laser for the treatment of acne scars: differential expression of fibrogenetic biomolecules may be associated with differences in efficacy between ablative and non-ablative laser treatment. Lasers Surg Med 2017; 49: 341–347.
21. Boen M, Jacob C. A review and update of treatment options using the acne scar classification system. Dermatol Surg 2019; 45: 411–422.
22. Moon J, Yoon JY, Yang JH, Kwon HH, Min S, Suh DH. Atrophic acne scar: a process from altered metabolism of elastic fibres and collagen fibres based on transforming growth factor-beta1 signalling. Br J Dermatol 2019; 181: 1226–1237.
23. Holland DB, Jeremy AH, Roberts SG, Seukeran DC, Layton AM, Cunliffe WJ. Inflammation in acne scarring: a comparison of the responses in lesions from patients prone and not prone to scar. Br J Dermatol 2004; 150: 72–81.
24. Alajlan AM, Alsuwaidan SN. Acne scars in ethnic skin treated with both non-ablative fractional 1,550 nm and ablative fractional CO2 lasers: comparative retrospective analysis with recommended guidelines. Lasers Surg Med 2011; 43: 787–791.
25. Sundaram H, Cegielska A, Wojciechowska A, Delobel P. Prospective, randomized, investigator-blinded, split-face evaluation of a topical crosslinked hyaluronic acid serum for post-procedural improvement of skin quality and biomechanical attributes. J Drugs Dermatol 2018; 17: 442–450.
26. Park GH, Rhee do Y, Moon HR, Won CH, Lee MW, Choi JH, et al. Effect of an epidermal growth factor-containing cream on postinflammatory hyperpigmentation after Q-switched 532-nm neodymium-doped yttrium aluminum garnet laser treatment. Dermatol Surg 2015; 41: 131–135.
27. Uaboonkul T, Nakakes A, Ayuthaya PK. A randomized control study of the prevention of hyperpigmentation post Q-switched Nd:YAG laser treatment of Hori nevus using topical fucidic acid plus betamethasone valerate cream versus fucidic acid cream. J Cosmet Laser Ther 2012; 14: 145–149.
28. Farkas JP, Richardson JA, Burrus CF, Hoopman JE, Brown SA, Kenkel JM. In vivo histopathologic comparison of the acute injury following treatment with five fractional ablative laser devices. Aesthet Surg J 2010; 30: 457–464.
29. Kwon HH, Choi SC, Lee WY, Jung JY, Park GH. Clinical and histological evaluations of enlarged facial skin pores after low energy level treatments with fractional carbon dioxide laser in Korean patients. Dermatol Surg 2018; 44: 405–412.
30. Choi JH, Shin EJ, Jeong KH, Shin MK. Comparative analysis of the effects of CO2 fractional laser and sonophoresis on human skin penetration with 5-aminolevulinic acid. Lasers Med Sci 2017; 32: 1895–1900.
31. Ha DH, Kim HK, Lee J, Kwon HH, Park GH, Yang SH, et al. Mesenchymal stem/stromal cell-derived exosomes for immunomodulatory therapeutics and skin regeneration. Cells 2020; 9: 1157.
32. Heo JS, Choi Y, Kim HO. Adipose-derived mesenchymal stem cells promote M2 macrophage phenotype through exosomes. Stem Cells Int 2019; 2019: 7921760.
33. Li X, Xie X, Lian W, Shi R, Han S, Zhang H, et al. Exosomes from adipose-derived stem cells overexpressing Nrf2 accelerate cutaneous wound healing by promoting vascularization in a diabetic foot ulcer rat model. Exp Mol Med 2018; 50: 29.
34. McBride JD, Rodriguez-Menocal L, Badiavas EV. Extracellular vesicles as biomarkers and therapeutics in dermatology: a focus on exosomes. J Invest Dermatol 2017; 137: 1622–1629.
35. Shin KO, Ha DH, Kim JO, Crumrine DA, Meyer JM, Wakefield JS, et al. Exosomes from human adipose tissue-derived mesenchymal stem cells promote epidermal barrier repair by inducing de novo synthesis of ceramides in atopic dermatitis. Cells 2020; 9: 680.
36. Hu L, Wang J, Zhou X, Xiong Z, Zhao J, Yu R, et al. Exosomes derived from human adipose mensenchymal stem cells accelerates cutaneous wound healing via optimizing the characteristics of fibroblasts. Sci Rep 2016; 6: 32993.
37. Kim WS, Park BS, Sung JH, Yang JM, Park SB, Kwak SJ, et al. Wound healing effect of adipose-derived stem cells: a critical role of secretory factors on human dermal fibroblasts. J Dermatol Sci 2007; 48: 15–24.
38. Wang L, Hu L, Zhou X, Xiong Z, Zhang C, Shehada HMA, et al. Exosomes secreted by human adipose mesenchymal stem cells promote scarless cutaneous repair by regulating extracellular matrix remodelling. Sci Rep 2017; 7: 13321.
39. Buch AS, Schjerling P, Kjaer M, Jorgensen LN, Krarup PM, Agren MS. Impaired collagen synthesis in the rectum may be a molecular target in anastomotic leakage prophylaxis. Wound Repair Regen 2017; 25: 532–535.
40. Kjaer M, Frederiksen AKS, Nissen NI, Willumsen N, van Hall G, Jorgensen LN, et al. Multinutrient supplementation increases collagen synthesis during early wound repair in a randomized controlled trial in patients with inguinal hernia. J Nutr 2020; 150: 792–799.
41. Lee JH, Ha DH, Go HK, Youn J, Kim HK, Jin RC, et al. Reproducible large-scale isolation of exosomes from adipose tissue-derived mesenchymal stem/stromal cells and their application in acute kidney injury. Int J Mol Sci 2020; 21: 4774.
42. Center for Biologics Evaluation and Research, Food and Drug Administration, U.S. Department of Health and Hu-

man Services. Guidance for industry: guidance for human somatic cell therapy and gene therapy. 1998. Available from: URL:https://www.fda.gov/media/72402/download
43. Center for Biologics Evaluation and Research, Food and Drug Administration, U.S. Department of Health and Human Services. Guidance for FDA reviewers and sponsors: content and review of chemistry, manufacturing, and control (CMC) information for human somatic cell therapy investigational new drug applications (INDs). 2008. Available from: URL:https://www.fda.gov/media/73624/download
44. Trivedi A, Miyazawa B, Gibb S, Valanoski K, Vivona L, Lin M, et al. Bone marrow donor selection and characterization of MSCs is critical for pre-clinical and clinical cell dose production. J Transl Med 2019; 17: 128.
45. Yi YW, Lee JH, Kim SY, Pack CG, Ha DH, Park SR, et al. Advances in analysis of biodistribution of exosomes by molecular imaging. Int J Mol Sci 2020; 21.
46. Thery C, Witwer KW, Aikawa E, Alcaraz MJ, Anderson JD, Andriantsitohaina R, et al. Minimal information for studies of extracellular vesicles 2018 (MISEV2018): a position statement of the International Society for Extracellular Vesicles and update of the MISEV2014 guidelines. J Extracell Vesicles 2018; 7: 1535750.
47. Zhang B, Yeo RWY, Lai RC, Sim EWK, Chin KC, Lim SK. Mesenchymal stromal cell exosome-enhanced regulatory T-cell production through an antigen-presenting cell-mediated pathway. Cytotherapy 2018; 20: 687–696.
48. Pittenger MF, Mackay AM, Beck SC, Jaiswal RK, Douglas R, Mosca JD, et al. Multilineage potential of adult human mesenchymal stem cells. Science 1999; 284: 143–147.
49. Yeo RWY, Lai RC, Tan KH, Lim SK. Exosome: a novel and safer therapeutic refinement of mesenchymal stem cell. J Circulating Biomarkers 2013; 1: 1–11.
50. Kordelas L, Rebmann V, Ludwig AK, Radtke S, Ruesing J, Doeppner TR, et al. MSC-derived exosomes: a novel tool to treat therapy-refractory graft-versus-host disease. Leukemia 2014; 28: 970–973.
51. Mendt M, Kamerkar S, Sugimoto H, McAndrews KM, Wu CC, Gagea M, et al. Generation and testing of clinical-grade exosomes for pancreatic cancer. JCI Insight 2018; 3.
52. O'Loughlin AJ, Woffindale CA, Wood MJ. Exosomes and the emerging field of exosome-based gene therapy. Curr Gene Ther 2012; 12: 262–274.
53. Qin J, Xu Q. Functions and application of exosomes. Acta Pol Pharm 2014; 71: 537–543.
54. Sun L, Xu R, Sun X, Duan Y, Han Y, Zhao Y, et al. Safety evaluation of exosomes derived from human umbilical cord mesenchymal stromal cell. Cytotherapy 2016; 18: 413–422.

Appendix S1

SUPPLEMENTARY MATERIAL

Generation of adipose-derived stem cell-conditioned medium

Human adipose-derived stem cells (ASC) from a healthy donor were collected by liposuction and immediately transferred into the cell culture facility. Donor eligibility and the quality of adipose tissue were assessed according to the guidelines of the Korean Ministry of Food and Drug Safety (MFDS). After isolating ASCs from the adipose tissue of a healthy donor, ASCs were sub-cultured at a density of 3,000 cells/cm^2 with 10% foetal bovine serum (FBS) containing Dulbecco's Modified Eagle's Medium (DMEM) (Thermo Fisher Scientific, Waltham, MA, USA) in a humidified atmosphere of 5% CO_2 in air at 37°C. Cells were harvested with porcine trypsin-ethylenediaminetetracetic acid (Thermo Fisher Scientific), and washed with Dulbecco's phosphate-buffered saline (PBS) (Thermo Fisher Scientific). Cell stocks of passage 4 were stored in liquid nitrogen (1,100,000 cells/ml/1 vial). The quality of ASCs was controlled by assessing the sterility test, mycoplasma test, cell viability, endotoxin test, and virus tests. The surface markers for ASCs were also determined by flow cytometry, including positive markers of CD31, CD73, CD105, and CD146. Adipogenic, chondrogenic, and osteogenic differentiation potencies of ASCs were also measured.

To generate the ASC-conditioned medium (CM), a cell stock was thawed and sub-cultured passage 7. ASCs at passage 7 were plated at a density of 6,000 cells/cm^2 and cultured with 10% FBS containing DMEM in a humidified atmosphere of 5% CO_2 in air at 37°C for 3 days up to 90% confluency. Cells were washed 3 times with PBS and supplemented with 1% L-glutamine (200 mM) (Thermo Fisher Scientific) and 1% sodium pyruvate (100 mM) (Thermo Fisher Scientific). The cells were further cultured for 24 h and the CM was collected.

Isolation and quantification of adipose tissue stem cell-derived exosomes

Adipose tissue stem cell-derived exosomes (ASCE) were isolated from the ASC-CM by tangential flow filtration (TFF) as previously described (18, 35). Briefly, the CM was filtrated through a 0.22-μm polyethersulfone membrane filter (Merck Millipore, Billerica, MA, USA) to remove non-exosomal particles, such as cells, cell debris, microvesicles, and apoptotic bodies. The CM was concentrated by TFF with a 500 kDa molecular weight cut-off filter membrane cartridge (GE Healthcare, Chicago, IL, USA), and buffer exchange was performed by diafiltration with PBS. Isolated ASCE were aliquoted into polypropylene disposable tubes and stored at –80°C until use. Before using, frozen ASCE were left at 4°C until completely thawed and were not frozen again. The purity of isolated exosomes was confirmed by measuring the amounts of negative markers for exosomes. The ASCs and ASCE were lysed with RIPA buffer (Cell Signaling Technology, Danvers, MA, USA), and their protein concentrations were measured by the bicinchoninic acid (BCA) protein assay (Thermo Fisher Scientific). Each lysate was analysed using human CANX/calnexin ELISA kit (LifeSpan Bioscience, Seattle, WA, USA) and human cytochrome c ELISA kit (Abcam, Cambridge, MA, USA), respectively, according to the manufacturer's instruction.

Nanoparticle tracking analysis

The characterization of ASCE was further performed according to the criteria suggested by the Minimal Information for Studies of Extracellular Vesicles 2018 (MISEV 2018) and the Korean MFDS. To determine the size distribution and particle concentration, ASCE diluted with PBS were analysed by nanoparticle tracking analysis (NTA) using a NanoSight NS300 (Malvern Panalytical, Amesbury, UK) equipped with a 642-nm laser. Exosomes, diluted with PBS to between 20 and 80 particles per frame, were scattered and illuminated by the laser beam and their movement under Brownian motion was captured for 20 s at a camera level of 16. Videos were analysed by the NTA 3.2 software with constant settings. To provide a representative result, at least 5 videos were captured and >2,000 validated tracks were analysed for each individual sample. The NTA instrument was regularly checked with 100 nm-sized standard beads (Thermo Fisher Scientific). To provide representative size distribution of exosomes, size distribution profiles from each video replicates were averaged. Exosome surface markers were analysed using bead-based flow cytometry. Briefly, ASCE were captured by Exosome Dynabead for human CD9, CD63, or CD81 (Invitrogen, Carlsbad, CA, USA), respectively, according to the manufacturer's instruction. Captured exosomes were incubated with phycoerythrin-conjugated anti-human CD9, CD63, CD81, or isotype antibody (BD Biosciences, Franklin Lakes, NJ, USA), respectively.

Cryo-transmission electron microscopy (cryo-TEM)

Cryo-TEM images were obtained using a BIO-TEM installed at the Korea Basic Science Institute (Osong, Republic of Korea). The isolated ASCE were applied to Quantifoil grids (Electron Microscopy Sciences, Hatfield, PA, USA) and subsequently blotted using Vitrobot Mark IV (FEI, Hillsboro, OR, USA) with the following settings: 100% humidity; 4°C; blot time of 5 s; blot force of 5; blot total of 1; wait time of 5 s; drain time of 0 s. For maintenance of vitrified sample grids at a temperature of approximately –178°C within the TEM, a side entry Gatan 626 cryo-holder (Gatan, Pleasanton, CA, USA) was used. The grids were then examined with a Tecnai G2 Spirit Twin TEM equipped with anti-contaminator (FEI). A 4K×4K, Ultrascan 4000 CCD camera (Gatan) was used for image recording. A low-dose method (exposures at 1,000 electrons per nm^2/s) was used for cryo-TEM.

In vitro *potency assay of adipose tissue stem cell-derived exosomes*

Isolated and quantified ASCE were tested *in vitro* for their potency in terms of collagen synthesis, inflammatory IL-6 reduction, cell migration, and cell proliferation. Human dermal fibroblasts (HDFs) were obtained from CEFO (Seoul, Republic of Korea) and cultured in Human Fibroblast Growth Medium with 10% supplements (CEFO), 100 IU/ml penicillin, and 100 μg/ml streptomycin in humidified atmosphere of 5% CO_2 at 37°C. For collagen assay, HDF cells were incubated with supplement-free medium for 24 h, followed by ASCE (7.8×10^{11} particles/ml) treatment. After 24-h incubation, the culture medium was collected and the amount of procollagen type I was measured according to the manufacturer's protocol using procollagen type I C-peptide EIA kit (Takara Bio, Inc., Otsu, Japan). For cell migration assay, a single wound was created by using IncuCyte® WoundMaker Tool (Essen Bioscience, Hertfordshire, UK) when HDF cells reached 90% confluency. The cells were cultured in supplement-free medium with ASCE (1×10^{11} particles/ml) for 24 h. The data were acquired and analysed by IncuCyte® S3 Live-Cell Analysis System and software (Essen Bioscience). For cell proliferation assay, HDF cells were plated at a density of 3,000 cells/cm^2. After 24 h, the culture medium was changed into growth medium with 1% supplement, and ASCE (3.3×10^{11} particles/ml) was treated. The cell proliferation was measured and analysed using IncuCyte® S3 Live-Cell Analysis System and software (Essen Bioscience). For anti-inflammation assay, the RAW 264.7 cells (ATCC, Manassas, VA, USA) were cultured in DMEM supplemented with 10% FBS, 100 IU/ml penicillin, and 100 μg/ml streptomycin in humidified atmosphere of 5% CO_2 at 37°C. The cells were incubated with ASCE (1.3×10^{11}

particles/ml) for 24 h, and stimulated by 100 ng/ml lipopolysaccharide (LPS). The cell culture supernatants were harvested 24 h after LPS stimulation and IL-6 level in the supernatants was analysed using the LEGENDplex™ Mouse Inflammation Panel (BioLegend, San Diego, CA, USA) according to the manufacturer's protocol. The data were acquired by NovoCyte Flow Cytometer System (ACEA Biosciences, Inc., San Diego, CA, USA) and analysed with LEGENDplex 8.0 software (BioLegend) (SFig. 1).

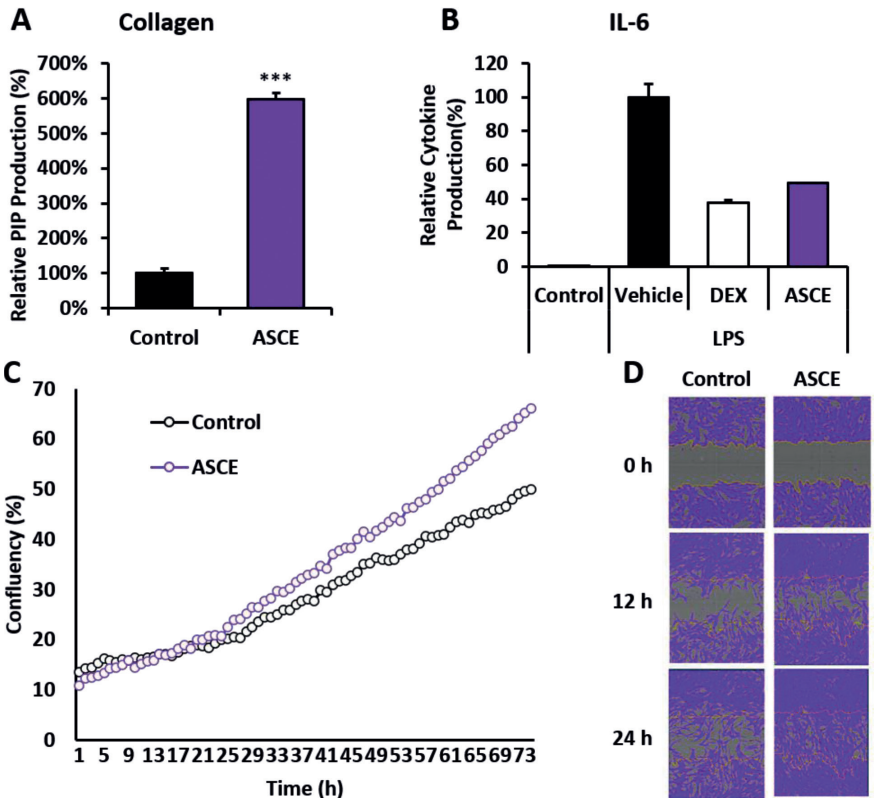

SFig. 1. *In-vitro* potency of adipose tissue stem cell-derived exosomes (ASCE). (A) Effects of ASCE on procollagen type I protein synthesis in human dermal fibroblast (HDFs). (B) Anti-inflammatory effects of ASCE in RAW 264.7 cells. (C) Effects of ASCE on HDF proliferation. (D) Effects of ASCE on HDF migration. Data are presented as mean ± standard deviation (SD); ***$p < 0.001$ compared with control. PIP: procollagen type I C-peptide; DEX: dexamethasone; LPS: lipopolysaccharide.

Determination of dose of adipose tissue stem cell-derived exosomes

Currently, no recommended dose of exosomes for human or animal is available (S1). Since this is the first clinical study that uses ASCE for human skin wound repair, we carefully chose the dose to be as high as possible. The median lethal dose cut-off value was higher than 1×10^{11} particles/kg in acute oral toxicity test performed in Sprague Dawley (SD) rats (S1). In addition, no observed effect level was calculated as over 1.07×10^{11} particles/kg/day in repeated dermal toxicity test performed in SD rats with daily dermal application for 13 weeks. Human equivalent dose (HED) was calculated by the equation of [HED (per kg)=animal dose (per kg)/conversion factor] (S2, S3). Since the conversion factor of rat is 6.17, the HED of ASCE (per 50 kg of person) was (1.07×10^{11} particles/kg/day)/$6.17\times$(50 kg)=8.67×10^{11} particles/day. According to the US FDA recommendation, the maximum recommended starting dose (MRSD) was calculated by the equation of [MRSD=HED/10] (S2, S3). Thus, the MRSD was (8.67×10^{11} particles/day)/10=8.67×10^{10} particles/day. Based on these calculations, we carefully chose the dose of ASCE for the day of fractional CO_2 laser (FCL) treatment as 9.78×10^{10} particles/ml (within $[8.67\pm1.73]\times10^{10}$ particles/day) with 20% error range in consideration of the loss during the treatment. For days subsequent to FCL treatment, we further reduced the dose of ASCE below 1/5 of MRSD to reduce any adverse effect that may be caused by repeated applications, and it was calculated as 1.63×10^{10} particles/ml (less than 20% of 8.67×10^{10} particles/day).

Composition of the adipose tissue stem cell-derived exosomes and control gel solution

The ASCE gel solution contained 30% ASCE, 2% 1,2-hexanediol (Cosbon Co., Ltd, Hwaseong, Republic of Korea), 1% glycerin (Procter and Gamble Chemicals, Cincinnati, OH, USA), 0.6% ammonium acryloyldimethyltaurate/VP copolymer (Clariant International Ltd, Muttenz, Switzerland), 0.0045% L-arginine (Daesang, Seoul, Republic of Korea), and 66.3955% water for injection (Dai Han Pharm. Co., Ltd, Seoul, Republic of Korea). Percentages refer to weight per weight. For the control agent, 30% of 0.03× PBS was used in the gel solution in place of the exosomes.

Statistical analysis

Percentage changes from baseline in total échelle d'évaluation clinique des cicatrices d'acné (ECCA) scores and changes in scores of 3 major subtypes (V-, U-, and M-shaped) of atrophic scars were analysed using linear mixed effect models that included treatment group, visit, and their interaction as fixed factors, and a random factor for subjects and crossed random effect terms for treatment group and visit nested within subject. Percentage changes from baseline in atrophic scar volume, mean pore volume, and skin surface roughness were assessed using linear mixed effect models which included treatment group, visit, and their interaction as fixed factors, and a random intercept at subject level. The duration of downtime was evaluated using a generalized linear mixed model with log link function and generalized Poisson family, which included the same fixed and random effects as those in the ECCA analyses. Post-treatment pain, erythema, oedema, and dryness were assessed using cumulative link mixed models with logit link function that included treatment group, post-treatment day, and their interaction as fixed factors, and random intercepts for subject and visit nested within the subject.

SUPPLEMENTARY REFERENCES

S1. Ha DH, Kim SD, Lee J, Kwon HH, Park GH, Yang SH, et al. Toxicological evaluation of exosomes derived from human adipose tissue-derived mesenchymal stem/stromal cells. Regul Toxicol Pharmacol 2020; 115: 104686.

S2. Nair AB, Jacob S. A simple practice guide for dose conversion between animals and human. J Basic Clin Pharm 2016; 7: 27–31.

S3. Shin JW, Seol IC, Son CG. Interpretation of animal dose and human equivalent dose for drug development. J Korean Oriental Med 2010; 31: 1–7.